ELSEVIER

Polymer 41 (2000) 335–349

polymer

Fracture behavior of nylon 6/ABS blends compatibilized with an imidized acrylic polymer

R.A. Kudva, H. Keskkula, D.R. Paul*

Department of Chemical Engineering and Texas Materials Institute, University of Texas at Austin, Austin, TX 78712, USA

Received 15 December 1998; accepted 17 March 1999

Abstract

The fracture behavior of blends of nylon 6 and acrylonitrile–butadiene–styrene (ABS) compatibilized with an imidized acrylic (IA) polymer was examined by Izod impact testing and single-notch three-point bend (SEN3PB) instrumented Dynatup tests. The effects of the method of fracture surface measurement, ABS content, specimen thickness, compatibilizer content and fracture zone geometry were investigated. Blends containing a fixed (5 wt.% IA) compatibilizer content were tough over a broad range of ABS contents; the optimum toughness occurred near 50 wt.% ABS. A dual-mode of fracture was observed in SEN3PB specimens whose Izod impact samples with the same composition had ductile–brittle transition temperatures near room temperature. In these SEN3PB samples, ductile deformation occurred in samples with shorter ligament lengths, whereas brittle failure prevailed in samples with longer ligament lengths. The critical ligament length at which the ductile-to-brittle transition occurs was shown to be dependent on the compatibilizer content and specimen thickness. These dual modes of fracture were rationalized in terms of a plane–strain to plane–stress transition. For blends that were super tough and had good low temperature toughness as judged by Izod impact testing, the toughness of SEN3PB specimens was generally insensitive to specimen thickness; these blends were fully ductile over the entire range of ligament lengths. The size of the stress-whitened zone was examined for fractured SEN3PB specimens that were fully ductile over the entire range of ligament lengths. Among specimens of a given composition, the size of the stress-whitened zones was geometrically similar and independent of the size of the original ligament. However, when ductile samples of different composition were compared, the size of the stress-whitened zone was not necessarily proportional to the energy dissipated during plastic deformation. This may be a result of the presence of different modes of energy absorption in the nylon 6 or SAN matrix phase.

Keywords: Nylon; Acrylonitrile–butadiene–styrene; Imidized acrylic polymer

1. Introduction

Blends of polyamides with acrylonitrile–butadiene–styrene (ABS) materials are of significant commercial interest. Polyamides provide good strength, stiffness and resistance to nonpolar solvents, whereas ABS materials provide toughness and low cost. Although simple blends of polyamides and ABS exhibit poor mechanical properties, their properties can be greatly improved, often with synergistic effects, through appropriate compatibilization [1–15]. The preferred method of compatibilization for these systems has been to incorporate a material that is miscible with the SAN phase of the ABS and also capable of reacting with nylon 6. Such strategies have been successful in developing super-tough blends [1–12].

The impact properties of such toughened materials are generally characterized by standard notched Izod impact testing. Although these tests are convenient and useful, they provide a limited picture of the fracture behavior of ductile materials. In this paper, the fracture behavior of compatibilized blends of nylon 6 and ABS are investigated in more detail using both notched Izod and instrumented Dynatup single-edge notched three-point bend (SEN3PB) impact tests. The compatibilizer used is an imidized acrylic polymer, which contains anhydride and acid functionalities capable of reacting with nylon 6 and has been shown to generate nylon 6/ABS blends that are super tough as judged by standard Izod impact testing [7–11]. The effects of the method of fracture surface measurement, ABS content, specimen thickness, compatibilizer content and stress-whitened zone geometry are examined to better understand their influence on the fracture behavior of these blends.

* Corresponding author. Tel.: +1-512471-5392; fax: +1-512471-0542.

0032-3861/00/$ - see front matter
PII: S0032-3861(99)00244-X

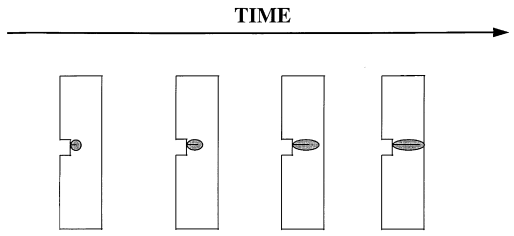

Fig. 1. Schematic of crack propagation through a SEN3PB during a Dynatup test. The stress-whitened zone advances ahead of the crack as it propagates.

2. Background

Most of the literature describing toughened multiphase plastics has relied on standard notched Izod impact testing to characterize toughness. These tests are quite useful in the plastics industry because of their convenience and ease of comparison of materials; however, they provide only limited information regarding the fracture behavior of ductile materials. The use of thin specimens and a standard notch often does not create sufficiently severe impact conditions to adequately discriminate among ductile blend systems. In addition, the standard Izod impact test provides the total fracture energy for only one notch depth, i.e. the ligament length, and notch radius.

There is growing interest in the use of fracture mechanics techniques, traditionally designed for testing metals, to characterize the toughness and understand the deformation processes that occur in toughened plastics [16–23]. However, techniques based on linear elastic fracture mechanics (LEFM) are not well suited to rubber-toughened materials, which can form extensive yield zones ahead of a propagating crack. The conditions of LEFM are empirically formulated to ensure that the test specimens are in a state of plane strain, which generally requires specimen thicknesses greater than what is practical for injection molding of plastic parts. The *J*-integral method has been regarded as more appropriate for characterizing ductile polymeric materials [24,25] because a plane–strain toughness value can be obtained with specimens that are smaller than necessary for LEFM. However, these tests require specialized equipment for the accurate measurement of slow stable crack growth, and the required thickness is still often beyond what can be conveniently fabricated.

Vu-Khanh [26] and Mai [27] have developed approaches to characterizing fracture behavior that do not require the rigorous treatment of fracture mechanics, yet provide more detailed characterization than conventional Izod tests. Each methodology involves a two-parameter model and originates from the ideas first proposed by Broberg [28,29], who stated that the region surrounding a crack tip can be partitioned into an end region where actual fracture occurs and an outer region where energy is plastically absorbed during crack propagation. Both of these methods have been employed to characterize a wide variety of ductile polymers and their blends [26,27,30–48]. Although both of these treatments have proven useful, there are fundamental differences in the interpretation of these two-parameter models, as well as in the loading configuration, testing speed and sample geometry. In the model proposed by Vu-Khanh [26], the energy required (U) to fracture ductile specimens (thickness $= t$) of varying ligament lengths (ℓ) is of the following form:

$$U/A = G_i + 1/2T_aA, \tag{1}$$

where $A = \ell t$ is the area of the ligament. The intercept, G_i, of a plot of U/A versus A has been called the fracture energy at crack initiation, whereas the term related to the slope T_a has been called the tearing modulus, a concept originally developed by Paris et al. [49,50]. The methodology proposed by Vu-Khanh employs high-speed loading of thick samples in bending.

The convention developed by Mai et al., known as the essential work of fracture (EWF) method, partitions the energy to break a specimen into an essential work in the fracture process zone and a nonessential work performed in the outer plastic zone [27,36–40]. The total energy absorbed in fracturing a specimen, W_f, is divided into two parts by the expression

$$W_f = w_e\ell t + w_p\beta\ell^2 t, \tag{2}$$

where w_e is the specific essential work of fracture (units of energy per unit area), β a geometry-dependent plastic zone shape factor and w_p the specific nonessential plastic work (units of energy per unit volume). The term containing w_e represents the energy required to create a unit area of fracture surface, whereas the term containing w_p corresponds to the dissipated energy per unit volume in the stress-whitened zone. Normalizing Eq. (2) by ℓt, the total specific work of fracture, w_f (units of energy per unit area), to fracture a ligament of length ℓ becomes

$$w_f = w_e + \beta w_p\ell. \tag{3}$$

According to this model, a plot of w_f versus ℓ should yield a straight line with intercept w_e and slope βw_p. The EWF method generally uses very thin specimens tested at slow speeds in uniaxial tension.

According to a recently established protocol, there are several important criteria that must be satisfied in order to apply the EWF methodology to evaluate fracture toughness [51]. One of these conditions is that the specimen ligament must be fully yielded before crack initiation. In order to determine if the current materials fit this criterion, several ductile specimens were tested such that the impact test was stopped immediately after crack initiation. In these samples, the crack had clearly advanced before full ligament yielding. By comparing samples with arrested cracks to more fully broken specimens, it appears that the stress-whitened zone advances ahead of the crack as it propagates, as represented in Fig. 1.

Table 1
Polymers used in this study

Polymer	Material/description	Composition	Molecular weight	Brabender torque[a] (Nm)	Source
Nylon 6	Capron 8207 F[b]	End-group content: $NH_2 = 47.9$ μeq/g $COOH = 43.0$ μeq/g	$\bar{M}_n = 22\,000$	7.3	Allied Signal
ABS	SAN-grafted emulsion rubber (Starex)	45% rubber 25% AN in SAN	$\bar{M}_n = 35\,000$[c] $\bar{M}_w = 90\,000$	20.1	Cheil Industries
IA	Imidized acrylic polymer (EXL 4140)	55.7 wt.% methyl glutarimide 41.0 gwt.% methyl methacrylate 2.2 wt.% methacrylic acid 1.1 wt.% glutaric anhydride	$\bar{M}_w = 95000$	9.8	Rohm and Haas

[a] Measurements taken at 240°C and 60 rev/min after 10 min.
[b] The designation of this material has recently been changed to B73WP.
[c] From g.p.c. using polystyrene standards; the information shown is for soluble SAN.

Another requirement is that the size of the outer plastic zone surrounding the fractured ligament must scale with the square of the ligament length. It will be demonstrated later that the current ductile blends satisfy this condition. In addition to the criteria stated above, Mai has recently noted that the EWF methodology may be difficult to apply if the two halves of the specimens are not completely separated after impact testing [52]. This issue is addressed with regard to the current materials in a later section.

In this study, the test conditions used are similar to those used by Vu-Khanh (thick specimens deformed in bending under high-speed loading) in order to discriminate among the current blends; however, the results will be shown using a presentation that is mathematically similar to the EWF method used by Mai et al. Recent work from this laboratory has shown that when comparing samples of different thicknesses, the specific fracture energy of polycarbonate/ABS blends is more closely related to the ligament length than its area [53]. It will be demonstrated later that comparing the specific fracture energy to the ligament length is a more appropriate basis for characterizing the current blends as well.

As the testing conditions and sample geometries used here may not fully comply with the yielding criterion established by the EWF method, we recognize that by plotting the normalized fracture energy versus the ligament length, the slope and intercept may not necessarily be equivalent to w_e and βw_p, respectively. Thus, in previous papers we have chosen to use a different nomenclature for the intercept and slope of the plots of w_f versus ℓ, i.e.

$$U/A = u_o + u_d\ell, \tag{4}$$

where U/A is the total fracture energy per unit area, ℓ the ligament length, u_o (units of energy per unit area) is called the limiting specific fracture energy and u_d is defined as the dissipative energy density (units of energy per unit volume), as it reflects plastic deformation energy in the process zone surrounding the fracture surface [53,54]. These should be regarded as phenomenological parameters where, in certain cases, the identifications $u_o = w_e$ and $u_d = \beta w_p$ are justified.

3. Experimental

Table 1 summarizes the relevant characteristics of the materials used in this study. Nylon 6 is a commercially available material with $\bar{M}_n = 22,000$ and a nearly equivalent amount of acid and amine end groups. The ABS material is an emulsion-made SAN grafted rubber concentrate containing 45 wt.% of nearly monodisperse butadiene rubber particles in the range of 0.3 μm in diameter. The blends were compatibilized with an imidized acrylic (IA) polymer, synthesized by the reactive extrusion of PMMA and methyl amine, which contains anhydride and acid groups capable of reacting with nylon 6. A more complete description of the compatibilizer and its potential reactions with nylon 6 are described elsewhere [11,55,56].

Blends in this study were prepared by simultaneous extrusion of all components in a Killion single-screw extruder ($L/D = 30$, 2.54 cm) at 240°C using a screw speed of 40 rev/min. The extrudate was injection molded into 3.18 or 6.35 mm thick impact test bars using an Arburg Allrounder injection molding machine. Some samples were milled down on both lateral surfaces to obtain thinner samples, which also removes any skin formed during injection molding. Test specimens were visually inspected for air bubbles and surface flaws; specimens with defects were discarded. All polyamide-containing materials were dried in a vacuum oven at 80°C for at least 16 h before each processing step. Other materials were dried for at least 12 h in a convection oven at 65°C.

Notched Izod impact measurements (ASTM D256) were made using 3.18 mm thick Izod bars with a TMI pendulum-type impact tester equipped with an insulated chamber for heating and cooling the specimens. Instrumented impact testing was performed using a Dynatup Drop Tower Model 8200 with a 10 kg weight and tup speed of 3.5 m/s, the same as that specified in the standard Izod test. Between 18 and 36 samples (half gate-end and half far-end) of the SEN3PB specimens were tested with ligament lengths generally ranging from 2 to 10 mm. A sharp notch was made by inserting a fresh razor blade into the root of the

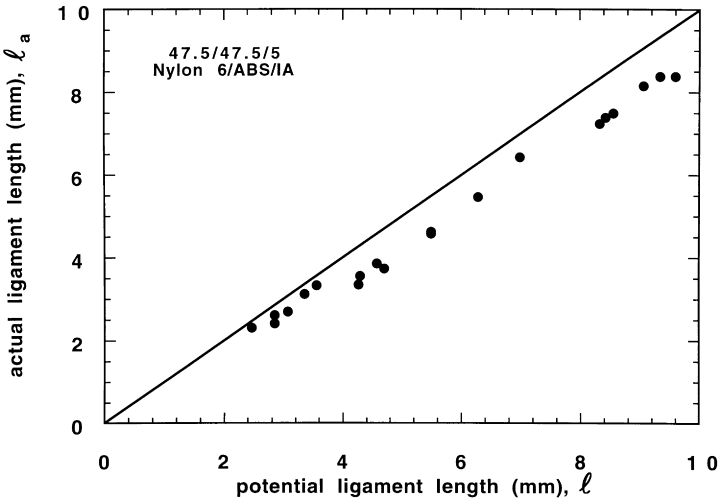

Fig. 2. Actual ligament length, ℓ_a, versus the potential ligament length, ℓ, for 47.5/47.5/5 nylon 6/ABS/IA SEN3PB specimens. The diagonal line represents the ideal case where the actual ligament length is equal to the potential ligament length.

notch. The total fracture energy was calculated from the integrated area under the load-deflection curves. Izod impact testing resulted in only partial breaks of the ductile materials used here; tests performed using the Dynatup for SEN3PB specimens generally led to more complete breaks. However, many of these SEN3PB samples were not completely broken after testing and consisted of unbroken ligaments that were generally 0.25–1.0 mm in length. A more complete description of the test apparatus, sample geometry, testing procedure and method of data analysis is provided elsewhere [34,57]. Blend morphologies were determined using a JEOL 200CX transmission electron microscope operating at an accelerating voltage of 120 kV. Samples were cryogenically microtomed into ultrathin sections (15–20 nm) from impact bars perpendicular to the flow direction. The sections were exposed to a 2 wt.% solution of phosphotungstic acid to stain the polyamide phase.

4. Fracture evaluation

The fracture behavior of uncompatibilized and compatibilized blends of nylon 6 and ABS are described here. The first section addresses the appropriate basis for measuring the fractured surface of SEN3PB specimens. The next section explores the effect of ABS content on fracture behavior at a fixed (5 wt.% IA = imidized acrylic polymer) compatibilizer content, whereas the following section describes the effects of sample thickness on the fracture behavior of some of these specimens. Then the effect of compatibilizer content on blend fracture properties is explored at a fixed ratio of nylon 6 to ABS (1:1). In the final section, the size of the stress-whitened zones of some materials are evaluated and related to their fracture properties.

4.1. Method of fracture surface measurement

It was mentioned earlier that even under the severe impact conditions imposed by the Dynatup, many of the ductile samples used here were not completely broken after the impact test. Thus, for these specimens, there is a slight difference between the ligament length based on the *potential* fracture surface (the distance from the end of the initial razor notch to the far edge of the bar) and that based on the *actual* fracture surface (which corresponds to the length that is actually fractured during the impact test). Thus, some consideration must be made regarding which method of fracture surface measurement should be used in the data analysis.

Fig. 2 shows a representative plot of the actual ligament length, ℓ_a, versus the potential ligament length, ℓ, for one of the ductile blends tested in the Dynatup; the diagonal line represents the ideal condition where the bar is completely broken during the impact test. These two lengths are slightly different but appear to be linearly related. Whether the actual or potential fracture surface should be used as a basis for measurement is arguable; however, using Eq. (4), all the normalized energy versus ligament plots describing the ductile specimens used here are linear, regardless of the convention used. There are no major differences in the slopes and intercepts of these plots, and the trends in toughness are the same when comparing different materials, independent of the method of fracture surface measurement. As the current results are not largely affected by the basis of measurement, unless noted otherwise, the plots in this study will be shown based on the potential fracture surface because it simplifies the analysis and offers a consistent

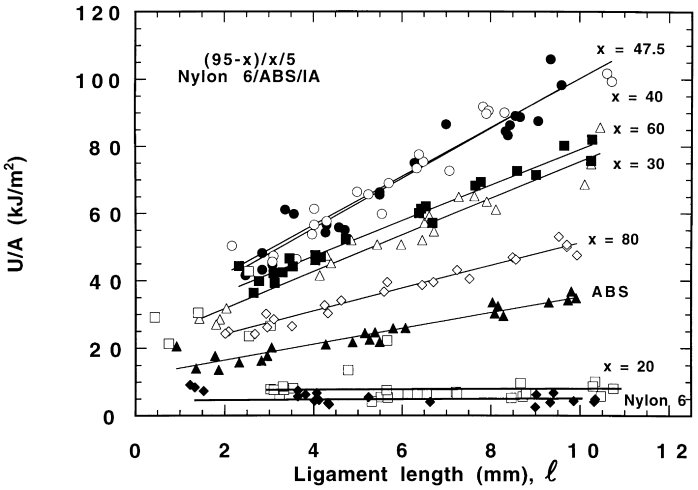

Fig. 3. Specific fracture energy as a function of the ligament length, ℓ, for nylon 6, ABS and (95-x)/x/5 nylon 6/ABS/IA blends for 6.35 mm thick specimens.

means of comparing the materials used here. An added justification of using the potential fracture surface is that to some extent it accounts for the energy absorbed in the small unbroken ligament (through bending, etc.) during the Dynatup test.

4.2. Effect of ABS content

The influence of the amount of ABS in the blend on the fracture behavior of SEN3PB specimens is described here. Excluding the pure nylon 6 and ABS controls, each of the blends contains a fixed (5 wt.% IA) compatibilizer content while the ratio of nylon 6 to ABS is varied. Fig. 3 shows the fracture energy per unit area (U/A) as a function of ligament length (ℓ) for 6.35 mm thick SEN3PB specimens. It is evident that the specific fracture energy is much higher for compatibilized blends over a broad range of ABS contents (30–80 wt.%) than for either nylon 6 or ABS alone; this synergism is at a maximum around 47.5 wt.% ABS. There appears to be a critical amount of ABS that is necessary to make these blends tough, as the blend containing 20 wt.% ABS is brittle over nearly the entire range of ligaments. Interestingly, the blend containing 20 wt.% ABS has a lot of scatter in the data, these samples fail in a ductile manner when the ligament length is short (less than 3 mm), whereas specimens with longer ligaments fail in a brittle manner. Similar dual modes of fracture (ductile–brittle) have also been observed in nylon 6/ethylene–propylene rubber blends [58] and poly(butylene terephthalate)/ABS blends [54]; this type of fracture behavior will be examined in more detail in a later section. Blends that are fully ductile over the entire range of ligament lengths (containing more than 20 wt.% ABS) exhibit a linear relationship between the specific fracture energy and ligament length, which allows for interpretation of these results in terms of Eq. (4).

The values of the specific limiting fracture energy, u_o, and the dissipative energy density, u_d, of the blends represented in Fig. 3 are shown in Fig. 4 as a function of ABS content. As most samples containing 20 wt.% ABS are brittle, values for u_o and u_d were calculated in the brittle region ($\ell > 3$ mm) in order to facilitate comparison with other blends. Among these blends, it appears there is some

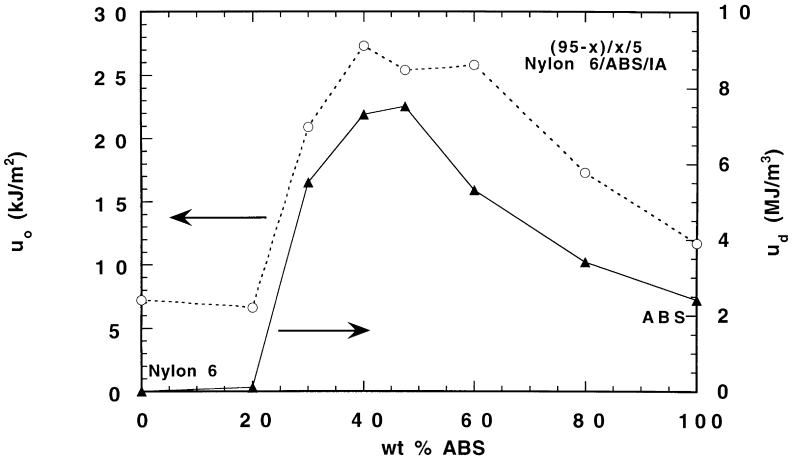

Fig. 4. Effect of ABS content on the specific limiting fracture energy, u_o, and the dissipative energy density, u_d, of the blends represented in Fig. 3.

Table 2
Izod and Dynatup values for blends with varying ABS contents

Composition	Izod impact values[a]		Dynatup impact values[b]	
	Room temperature impact strength (J/m)	Ductile–brittle transition temperature (°C)	u_o (kJ/m^2)	u_d (MJ/m^3)
Nylon 6	50	50	7.2	0.0
Nylon 6/ABS/IA blends (wt/wt/wt)				
75/20/5	572	22.5	6.6	0.1
65/30/5	851	−2.5	20.9	5.5
55/40/5	863	−25	27.3	7.3
47.5/47.5/5	974	−40	25.4	7.5
35/60/5	822	−45	25.8	5.3
15/80/5	613	−55	17.3	3.4
ABS	432	−70	11.7	2.4

[a] For 3.18 cm thick bars with a standard notch.
[b] For 6.35 cm thick bars with a sharp notch.

positive correlation between u_o and u_d. Both parameters are higher in most of the blends than in nylon 6 or ABS alone, with a maximum in both u_o and u_d when the blends contain equal parts of nylon 6 and ABS.

A comparison of the Dynatup impact parameters shown in Fig. 4 and the Izod impact values (room temperature impact strength and ductile–brittle transition temperature) of 3.18 cm bars with a standard notch is shown in Table 2. Despite the differences in sample thickness, test configuration and notch geometry, there are some interesting relationships between the Izod and Dynatup values. The value of u_d appears to become positive when the ductile–brittle transition temperature based on Izod tests drops below room temperature. The values of u_d and the room temperature impact strength reach a maximum at the same composition (47.5 wt.% ABS), and both decrease as the ABS content is increased. It is important to note that although compatibilized blends containing 30–60 wt.% ABS are super tough as judged by Izod impact testing (impact strengths > 800 J/m), the Dynatup test better discriminates the energy absorbed by plastic deformation, as indicated by the u_d values of these materials.

4.3. Effect of specimen thickness

The effect of thickness on the fracture behavior of SEN3PB Dynatup specimens is examined here using some of the blends described in the previous section. Fig. 5 shows the specific fracture energy versus the ligament length, ℓ, for specimens of 75/20/5 nylon 6/ABS/IA blends of different thicknesses. Fig. 5(a) represents on an expanded scale the same data shown in Fig. 3 for the blend with $x = 20$. As mentioned earlier, the mode of fracture in this material is dependent on the ligament length; samples with short ligaments deform in a ductile manner, whereas blends with longer ligaments fail in a brittle fashion. The ductile specimens could easily be identified by observation of a stress-whitened zone surrounding the fracture surface, as well as the higher specific fracture energy values relative to brittle samples (as seen in Fig. 5). This material exhibits brittle or ductile fracture depending on the ligament length and sample thickness; consequently, the specific fracture energy does not depend on the ligament length, as expected from Eq. (4). As the specimen thickness decreases, the critical ligament length at which this ductile–brittle transition occurs shifts to higher values. To emphasize this point, the failure mode of these materials is plotted as a function of ligament length and sample thickness in Fig. 6. It is evident that the thinnest specimens (3.18 mm thick) are ductile over nearly the entire ligament range, whereas the thickest specimens (6.35 mm thick) are ductile for only very short ligament lengths.

The fracture behavior of these materials can be rationalized in terms of the competition between yield and fracture in these SEN3PB specimens. Fig. 7 shows a simplified schematic of a SEN3PB specimen of width W containing a crack of length a; note that $\ell = W - a$. The stress level at which the net section can yield (σ_{max}) can be expressed as

$$\sigma_{max} = \sigma_y \left[\frac{W - a}{W} \right]^2 = \sigma_y \left[\frac{\ell}{W} \right]^2, \quad (5)$$

where σ_y represents the yield stress of an uncracked specimen [59]. As an approximation, the fracture stress, σ_f, can be expressed by rearranging the equation for fracture toughness as follows:

$$\sigma_f = \frac{K_c}{Y\sqrt{a}} = \frac{K_c}{Y\sqrt{W - \ell}}, \quad (6)$$

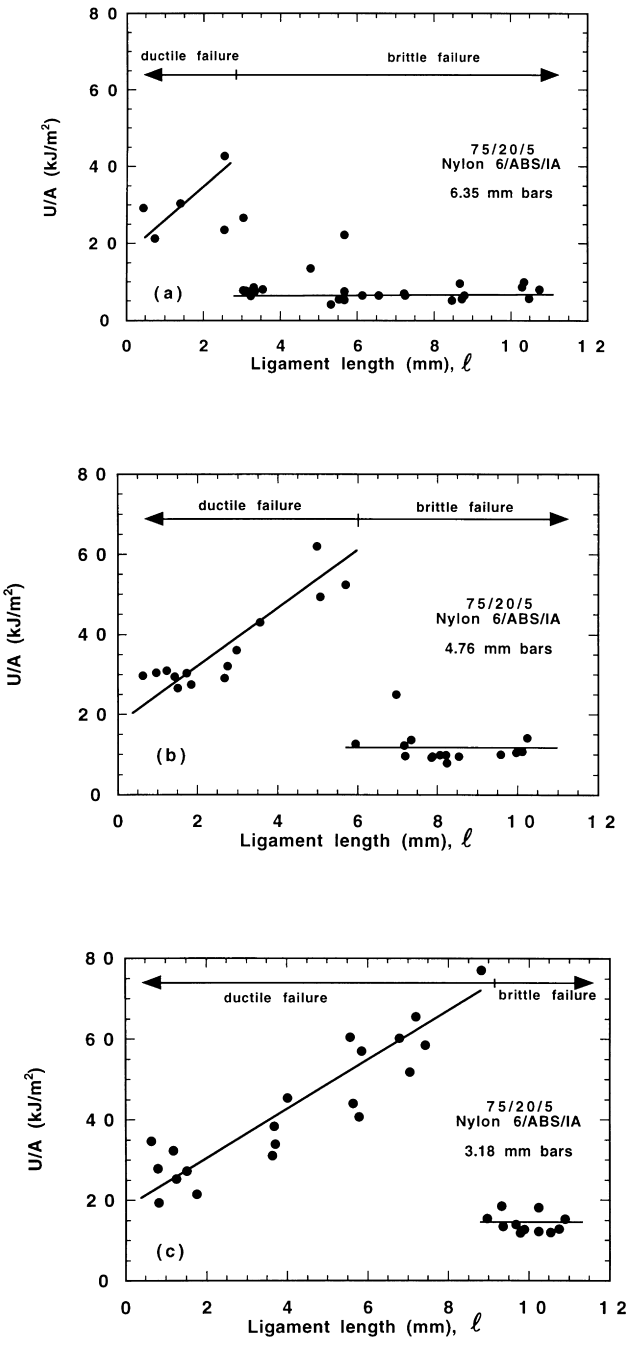

Fig. 5. Specific fracture energy as a function of the ligament length for 75/20/5 nylon 6/ABS/IA samples of varying thickness: (a) 6.35 mm; (b) 4.76 mm; and (c) 3.18 mm.

where K_c is the fracture toughness and Y a calibration factor that is a function of (a/W). The fracture toughness, K_c, decreases with increasing specimen thickness to a critical value, thereby representing plane–strain fracture conditions, or K_{Ic} [60,61]. As Eq. (6) has its foundations in LEFM, it may not be strictly valid for the present case; however, it conceptually provides a representation of modes of fracture.

Fig. 7 also provides a qualitative plot of failure stress versus ligament length, ℓ, for the specimens represented in Figs. 5 and 6; the shapes of the yield and fracture curves are drawn according to Eqs. (5) and (6). To simplify the current analysis, the calibration factor Y is considered constant because it is not a function of specimen thickness and does not influence the shapes of the fracture curves relative to each other. The observed mode of fracture in these specimens is governed by the relationship between the yield and fracture stresses for a given crack length and specimen thickness. When the fracture stress is lower than the yield stress, the sample will deform in a brittle manner. Conversely, when the yield stress is lower than the fracture stress, ductile failure will occur. As seen in Fig. 7, the stress at which samples break by yielding is not a function of the sample thickness (see Eq. (5)); however, the stress at which samples fail by brittle fracture decreases with increasing thickness as it is proportional to the fracture toughness (Eq. (6)). Thus, as the specimens become thicker and more nearly approach plane–strain conditions, i.e. as K_c decreases towards K_{Ic}, the yield and fracture curves intersect at shorter ligament lengths. Thus, thick specimens exhibit ductile failure only at short ligament lengths, whereas thinner specimens show ductile failure at longer ligament lengths. This provides a qualitative explanation for the trends observed in Fig. 5.

It is important to note that the blend composition described above has a ductile–brittle transition temperature near room temperatures as judged by Izod impact testing; thus, the mode of fracture in this “transition” material is quite sensitive to changes in specimen thickness and ligament length. Super-tough materials with ductile–brittle transition temperatures well below room temperature are not expected to be as strongly affected by such changes in specimen geometry. To demonstrate this, the effect of specimen thickness on the fracture behavior of a super-tough composition (47.5/47.5/5 nylon 6/ABS/IA) was explored. Fig. 8 shows the specific fracture energy versus the ligament length for 3.18 and 6.35 mm SEN3PB bars for this material. It appears that sample thickness only mildly affects the specific fracture energy for a given ligament size. All samples exhibited ductile fracture, regardless of the sample thickness or ligament length. In terms of the competition between yield and fracture, described in Fig. 7, this would imply that the fracture toughness (K_c) of these blends is sufficiently high that the fracture stress is greater than the yield stress over the entire range of ligaments and specimen thicknesses. Thus, the observed mode of failure is ductile, i.e. yielding occurs.

As the slopes of plots of the specific fracture energy versus the ligament length are relatively independent of the sample thickness for this fully ductile blend, it follows that their fracture responses would have quite different slopes if plotted versus the ligament area, $A = \ell t$. This suggests that under the current testing conditions, the fracture energy of these fully ductile materials is more closely a function of the ligament length than ligament area. This

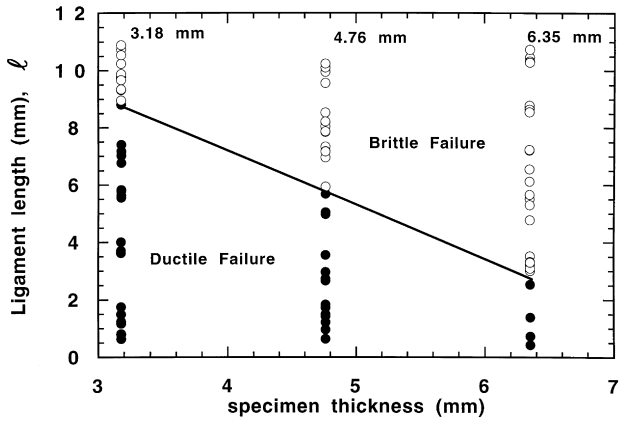

Fig. 6. Failure mode map for 75/20/5 nylon 6/ABS/IA blends represented in Fig. 5 as a function of the ligament length and specimen thickness.

observation is consistent with previous work from this laboratory that compared polycarbonate/ABS blends of different thicknesses [53].

One must consider that the fracture energies of blends represented in this study may be affected by the oriented skin layer of these injection molded specimens. Previous work has indicated that the blend morphology near the molded surface can be quite different from the morphology closer to the center of the bar and thus may be a factor influencing blend toughness [58]. To explore whether the "skin" affects the fracture behavior of the current specimens, the sides of 6.35 mm bars were machined off to yield 3.18 mm thick bars. The fracture behavior of these bars with no skin were then compared with the data for as-molded 3.18 mm thick bars (see Fig. 8). The plot of the specific fracture energy versus ligament length shown in Fig. 9 reveals no significant differences between these two types of 3.18 mm thick bars, i.e. the skin effects have little influence on the fracture behavior of these blends.

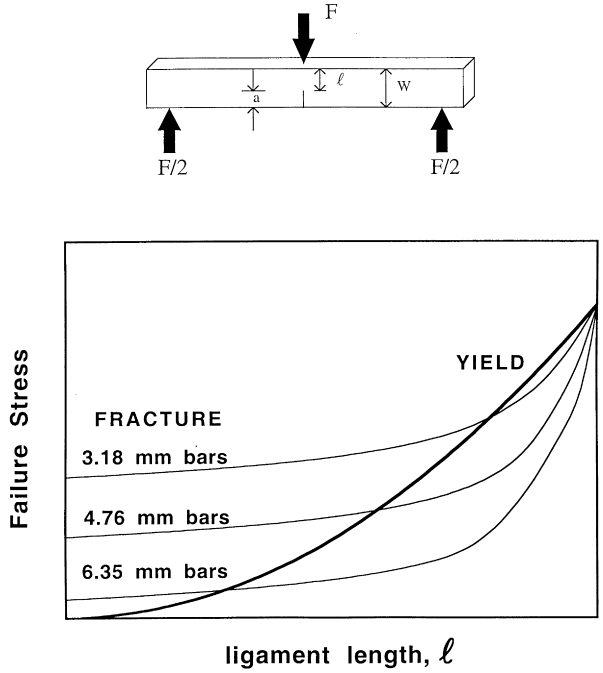

Fig. 7. Schematic of SEN3PB specimen of thickness W and containing a crack of length a, where $\ell = W - a$ and a qualitative representation of the failure stress (yield stress and fracture stress) versus the crack length in SEN3PB specimens. The yield stress is independent of specimen thickness, whereas the fracture stress decreases with increasing thickness. The shapes of the yield and fracture curves are drawn according to Eq. (5) and (6), respectively.

4.4. Effect of compatibilizer content

The effect of the amount of IA compatibilizer on the fracture properties of blends containing equal parts of nylon 6 and ABS is explored here. Plots of the specific fracture energy versus ligament length for 6.35 mm thick SEN3PB specimens are shown in Fig. 10 for blends containing different IA levels. The blends containing 1 wt.% or less of IA exhibit dual modes of failure and are not described by Eq. (4). The critical point, at which this ductile-to-brittle transition occurs, shifts to longer ligament lengths as the compatibilizer content is increased. The effect of increasing the compatibilizer content is qualitatively similar to the effect observed when the specimen thickness is decreased for some of the blends described in the previous section. In light of this observation, it appears that incorporating the compatibilizer serves to make plane–stress conditions more prevalent in a manner similar to decreasing the specimen thickness.

When the compatibilizer content is increased to 2 wt.%, the blends are fully ductile over the entire range of ligament lengths. Further increases in compatibilizer content do not appear to have a dramatic effect on the specific fracture energy for a given ligament length. Fig. 11 shows the limiting specific fracture energy, u_o, and the dissipative energy density, u_d, for the fully ductile blends obtained from simple linear regression analysis of the data in Fig. 10. The results show that when the compatibilizer content is increased, u_o increases while u_d decreases. This suggests that the energies absorbed in the inner and outer process zones do not necessarily change in the same direction, as in Fig. 4, when comparing different ductile specimens. However, before giving much physical interpretation to these trends, it is important to consider the statistical significance of these parameters because the data show some scatter. Fig. 12 shows a plot of the acceptable range of u_o and u_d values for two blends (containing 2 and 10 wt.% IA, respectively); the acceptable ranges, which are shown as ellipses, represent the joint 95% confidence regions for the values of u_o and u_d and enclose the values regarded as jointly reasonable for these parameters. This method takes into account the correlation between the best-fit estimates of u_o and u_d, shown in Fig. 11 [62,63], which are represented as dots in the centers of the two ellipses. Although there is a small range of acceptable u_d values that are common to both data sets (approximately 6.9–7.2 MJ/m^3), it is evident that the

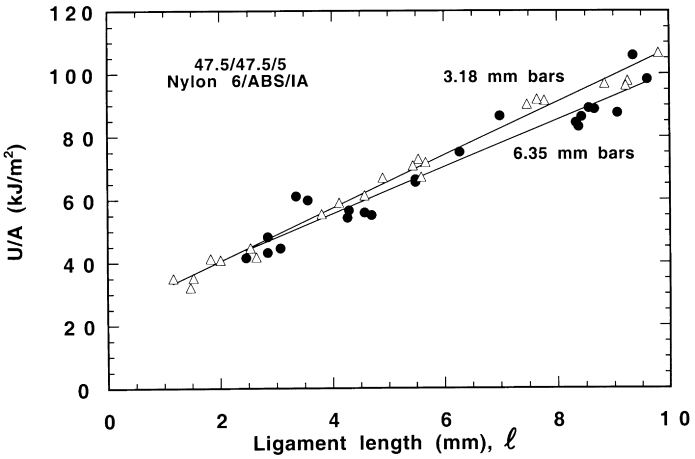

Fig. 8. Specific fracture energy as a function of the ligament length for 3.18 mm thick (▲) and 6.35 mm thick (●) specimens formed from the 47.5/47.5/5 nylon 6/ABS/IA blend.

ranges for the u_o values are quite different. Thus, it appears that the reduction in u_o with increasing compatibilizer content is quite real, but the changes in u_d may not be as significant as Fig. 11 might suggest. It is important to note that the two confidence regions (ellipses) in Fig. 12 do not intersect. This implies that the differences in the fracture data for these blends, albeit small (see Fig. 10), are indicative of real differences in the fracture behavior of these materials.

Table 3 shows a summary of the Dynatup results for blends described in Fig. 10, along with Izod impact data (room temperature impact strength and ductile–brittle transition temperature) obtained using 3.18–cm bars with a standard notch. All the compatibilized blends are super tough at room temperature as judged by Izod impact testing; however, the use of more severe conditions in the Dynatup allows for better discrimination among these ductile materials. As observed in blends where the nylon 6/ABS ratio is varied, there appears to be some relationship between the ductile–brittle transition temperatures of these blends (as judged by Izod impact testing) and the composition at which the corresponding SEN3PB samples become fully ductile in the Dynatup test. Blends with ductile–brittle transition temperatures far below room temperature (2 wt.% IA and higher) show ductile behavior over the entire range of ligaments in the SEN3PB test, whereas blends with ductile–brittle transition temperatures near or above room temperature (0 or 0.5 wt.% IA) exhibit dual modes of fracture and are not described by Eq. (4). Blends containing 1 wt.% IA appear to be an intermediate case, where the ductile–brittle transition temperature is below room temperature (but not as low as blends with higher IA contents) and ductile behavior is observed at all but very long ligament lengths.

4.5. Fracture zone geometry

The size of the stress-whitened zone formed during impact testing is an important consideration affecting the toughness of ductile polymers. In this section, the geometry

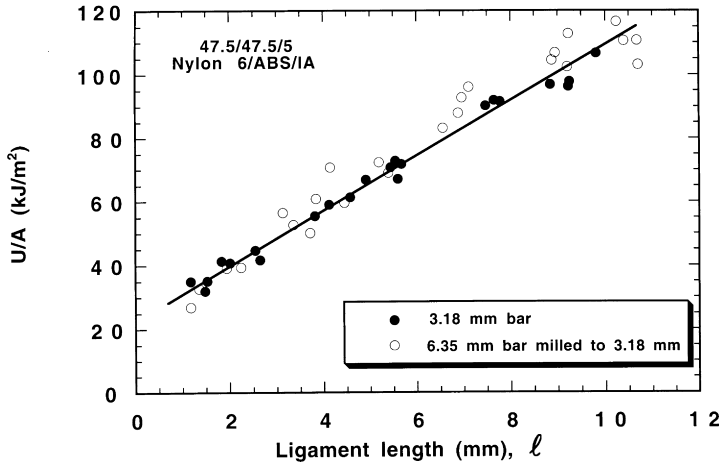

Fig. 9. Specific fracture energy as a function of the ligament length of 47.5/47.5/5 nylon 6/ABS/IA blends for as-molded 3.18 mm thick samples versus 6.35 mm thick samples machined down to 3.18 mm thickness.

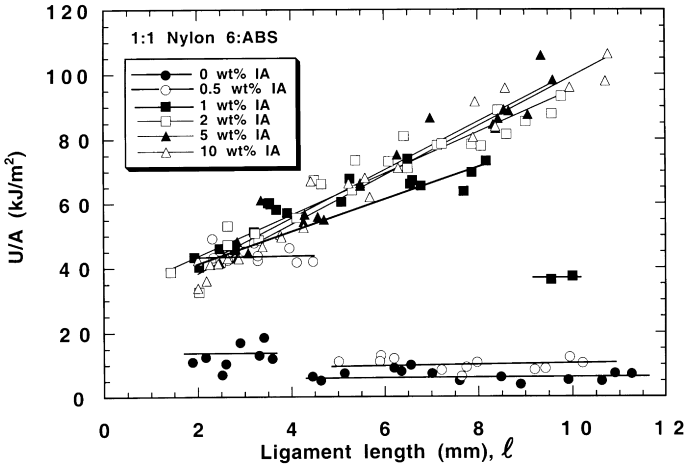

Fig. 10. Specific fracture energy as a function of the ligament length for nylon 6/ABS/IA blends of varying IA content. The ratio of nylon 6 to ABS is fixed at 1:1.

of the stress-whitened zones is explored for many of the current ductile materials.

Fig. 13 shows a schematic of a SEN3PB specimen after fracture in the Dynatup that is representative of the blends depicted here. The whitened zones of the specimens are elliptical in nature and are characterized here by their height, s, and the actual ligament length, ℓ_a. The shapes of these whitened zones were symmetric, i.e. the maximum height, s, is obtained at the center of the ligament. As noted earlier, these ductile specimens are generally not fully broken after the impact test, so the actual ligament length does not extend to the end of the bar. In this section, the actual ligament length, ℓ_a, is used instead of the potential ligament length because the ratio of s/ℓ_a more adequately represents the size of the stress-whitened zone. Fig. 14 shows the s/ℓ_a ratio as a function of the actual ligament length for several of the ductile SEN3PB specimens from Fig. 3. It is clear that the size of the stress-whitened zone varies among these different ductile materials. However, in all cases, the ratio of s/ℓ_a is independent of the size of the ligament; that is, the stress-whitened zones for a particular material are geometrically similar. As the s/ℓ_a ratio is constant for these specimens and the area of these stress-whitened zones are proportional to the product of s and ℓ_a, it follows that the size of these stress-whitened zone scales with the square of the ligament length. It is important to note that for the ductile specimens described here, the size of the stress-whitened zone is the same at the center as at the surface, i.e. s/ℓ_a does not vary in the through-thickness direction. Thus, the total volume of the elliptical stress-whitened zones for both halves of the broken specimen, V, can be expressed as

$$V_{swz} = \frac{\pi}{2} s \ell_a t, \tag{8}$$

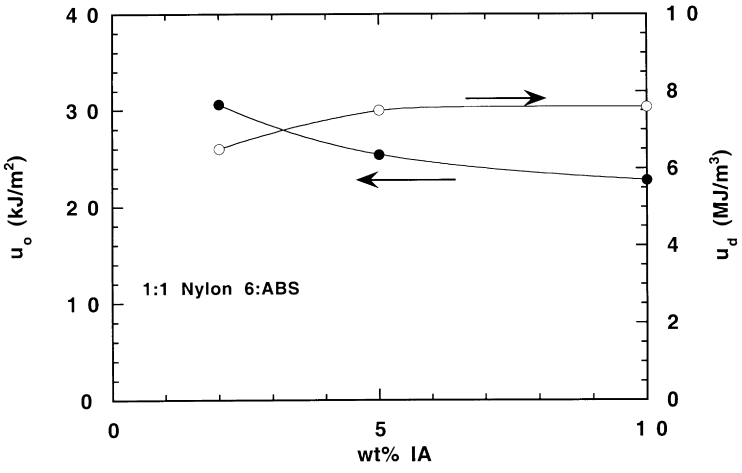

Fig. 11. Effect of IA compatibilizer content on the specific limiting fracture energy, u_o, and dissipative energy density, u_d, of nylon 6/ABS/IA blends. The ratio of nylon 6 to ABS is fixed at 1:1.

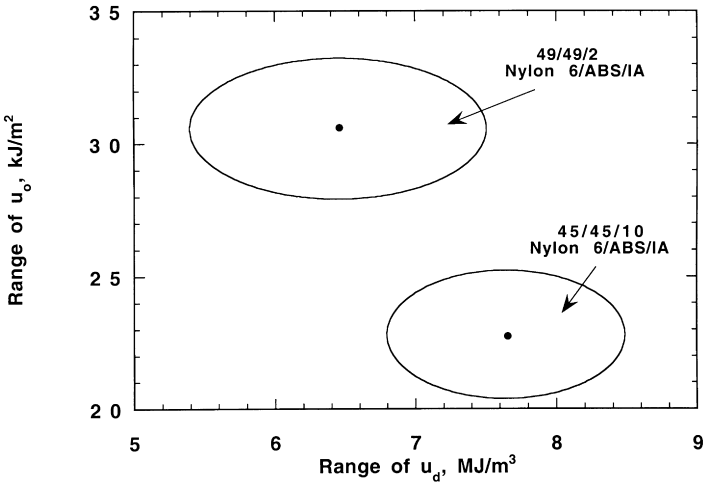

Fig. 12. Acceptable range of u_o and u_d values for 49/49/2 and 45/45/10 nylon 6/ABS/IA blends. The ellipses represent 95% joint confidence intervals for the u_o and u_d values shown in Fig. 11, based on their data in Fig. 10, and enclose the values of these parameters considered jointly reasonable. The points in the centers of the ellipses represent the best-fit u_o and u_d values based on the data in Fig. 10.

or equivalently

$$V_{swz} = \beta \ell_a^2 t, \tag{9}$$

where β is a constant equal to $(\pi/2)(s/\ell_a)$ and t the specimen thickness. Mai and others have noted that in order to obtain a linear relationship between the specific fracture energy and ligament length, the volume of the stress-whitened zone must scale with the square of the ligament length [51,52]. Here, it is demonstrated that the current materials fit this criterion.

Given the mathematical convention used in Eq. (4), the energy dissipated within the stress-whitened zone (U_{swz}) can be expressed as

$$U_{swz} = u_d \ell_a A = u_d \ell_a^2 t. \tag{10}$$

An expression for the energy absorbed per unit volume in the stress-whitened zone $(U/V)_{swz}$ can then be developed by dividing Eq. (10) by Eq. (8), which yields

$$\left(\frac{U}{V}\right)_{swz} = \frac{2}{\pi}\frac{u_d}{s/\ell_a} = \frac{u_d}{\beta}. \tag{11}$$

Thus, the ratio u_d to s/ℓ_a quantifies the energy dissipated per unit volume of stress whitened material. A plot of u_d versus s/ℓ_a can provide useful information regarding the amount of energy absorbed per unit volume among different ductile materials; Fig. 15 shows such a plot for several of the blends from Fig. 3. In the present case, values of u_d were based on the actual fractured ligament length and area; however, a qualitatively similar result is obtained when the potential fracture surface is the basis for evaluation of u_d. In this series, the compatibilizer content is fixed at 5 wt.%, whereas the ratio of nylon 6 to ABS is varied over the broadest range possible. These data are bounded by two straight lines drawn through the origin, corresponding to nylon 6, which exhibits no stress whitening in this test. One line represents

Table 3
Izod and Dynatup values for blends with varying compatibilizer contents

Nylon 6/ABS/IA (wt/wt/wt)	Izod impact values[a]		Dynatup impact values[b]	
	Room temperature impact strength (J/m)	Ductile–brittle transition temperature (°C)	u_o (kJ/m^2)	u_d (MJ/m^3)
50/50	141	35	n.c[c]	n.c.
49.75/49.75/0.5	931	15	n.c.	n.c.
49.5/49.5/1	960	−5	n.c.	n.c.
49/49/2	954	−35	30.6	6.5
47.5/47.5/5	974	−40	25.4	7.5
45/45/10	971	−50	22.8	7.6

[a] For 3.18 mm thick bars with a standard notch.
[b] For 6.35 mm thick bars with a sharp notch.
[c] n.c. = not calculated (as a dual mode of fracture was observed).

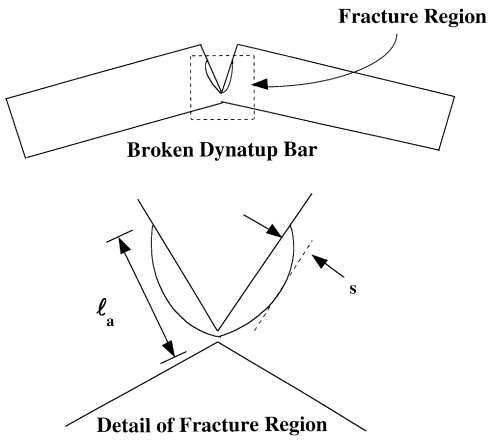

Fig. 13. Schematic of broken SEN3PB specimen indicating the actual ligament length, ℓ_a, and the height of the stress-whitened zone, s.

data for blends that contain up to 47.5 wt.% ABS; the other line represents data for blends containing 80% or more ABS. As seen in Fig. 16(a), ABS is the dispersed phase in the blend containing 47.5 wt.% ABS, whereas, the ABS domains are co-continuous when the ABS content is increased to 60 wt.% (see Fig. 16(b)). Other micrographs not shown here reveal that the blend compositions outside this range are clearly polyamide-continuous or ABS-continuous. From these observations, it appears that the upper line in Fig. 15 represents blends where nylon 6 is the continuous phase, whereas the lower line represents blends where ABS is the continuous phase. Blends with co-continuous phases of nylon 6 and ABS show an intermediate relationship.

It is evident that the amount of energy dissipated per unit volume of stress whitened material is greater in the nylon-continuous compositions, as indicated by the higher slope of this line (see Eq. (11)). It is interesting to note that pure ABS and the blend containing 30 wt.% ABS have stress-whitened zones nearly identical in size, as indicated by their s/ℓ_a ratios, yet the u_d value for the blend containing 30 wt.% ABS is much higher. As mentioned earlier, for each blend shown here, the size of the stress-whitened zone is the same in the center as at the fracture surface. Thus, the current results are not complicated by how thickness affects the size of the stress-whitened zone.

A more direct comparison of the energy dissipated per unit volume of the stress-whitened zone in these blends is provided in Fig. 17, where $(U/V)_{swz}$ is calculated by Eq. (11). For the material containing 20 wt.% ABS, which exhibits a dual mode of failure, the brittle samples exhibit no stress whitening, and thus the energy absorbed in this region is zero. Ductile samples of this composition have a finite $(U/V)_{swz}$ value, as calculated from the best-fit line through the ductile region in Fig. 5(c). As the ABS content is increased beyond 20 wt.%, the energy dissipated per unit volume remains relatively constant when the polyamide phase is continuous, decreases near the point of phase inversion and then reaches another constant, but lower, value when ABS becomes the continuous phase.

The different levels of energy absorption per unit of stress whitened volume (and thus variation of u_d for blends with similar plastic zone sizes) may stem from the different deformation mechanisms for the nylon 6 and SAN matrices. Considerable empirical evidence has shown that the sequence of events leading to energy absorption in rubber-toughened polyamides is cavitation of the rubber particles, which triggers subsequent shear yielding of the polyamide matrix [33,35,64–69]. Macroscopic specimens of ABS, however, tend to fail by a combination of shear yielding and crazing of the SAN matrix [70–75]. Among the current specimens, the polyamide-rich materials should have a greater tendency for energy absorption by the former mechanism, whereas ABS-rich materials will have a greater tendency for the latter. In the current case, it appears that more energy is dissipated per unit volume in blends that show significant shear yielding of the nylon 6. This

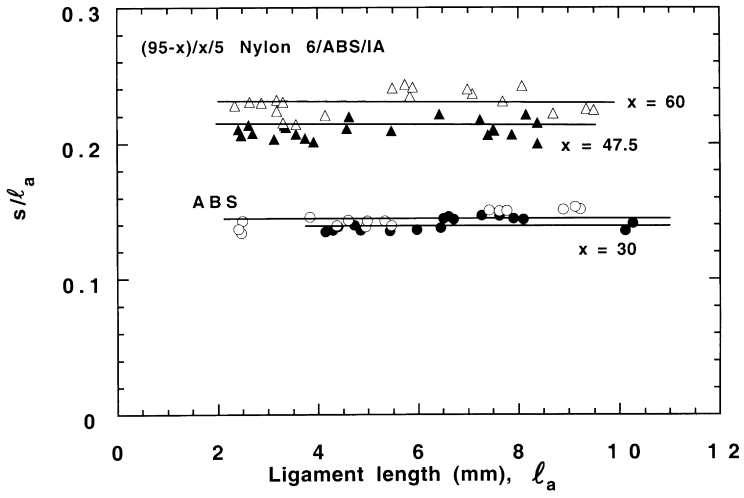

Fig. 14. Size of stress-whitened zone, represented by s/ℓ_a, versus the actual ligament length, ℓ_a, for ABS and (95-x)/x/5 nylon 6/ABS/IA blends.

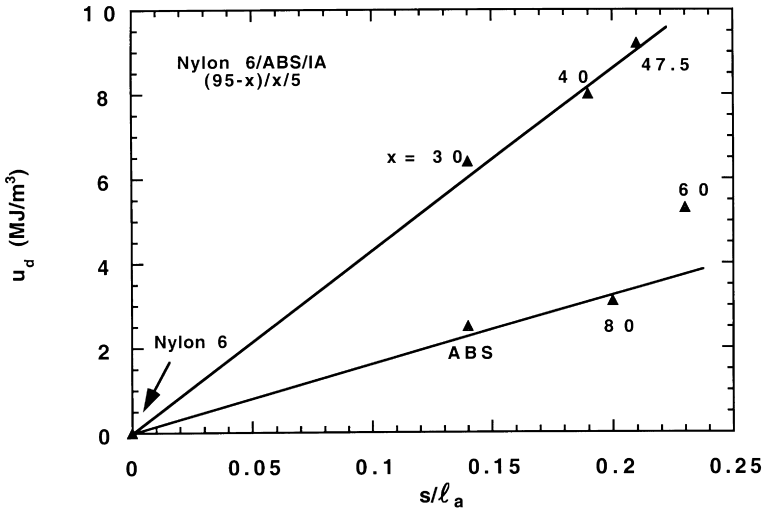

Fig. 15. Dissipative energy density, u_d, versus s/ℓ_a, for nylon 6, ABS and (95-x)/x/5 nylon 6/ABS/IA blends.

possibility has important ramifications with regard to designing toughened materials. Apparently, both the size of the yield zone and the preferred mode of energy absorption should be considered when developing toughened polyamide-based materials.

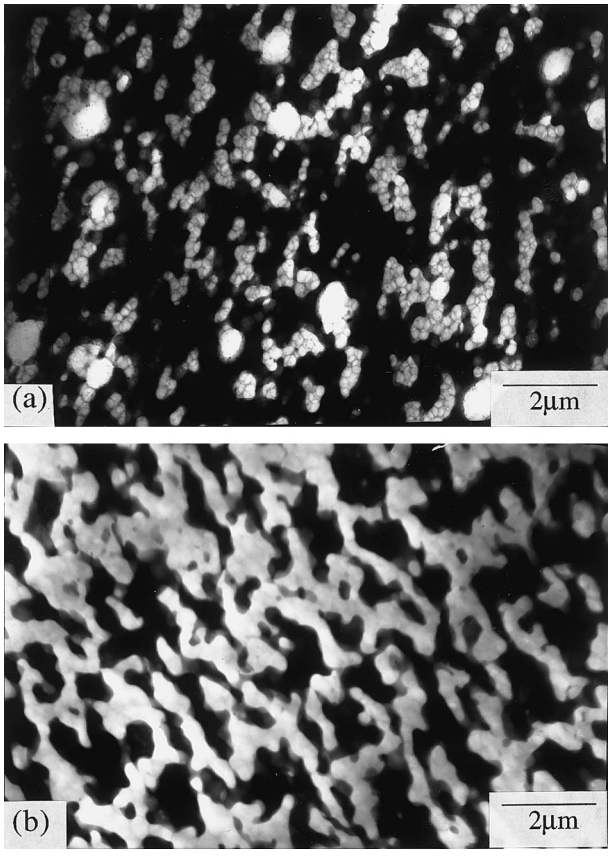

Fig. 16. TEM photomicrographs of nylon 6/ABS/IA blends of varying compositions; (a) 47.5/47.5/5 nylon 6/ABS/IA and (b) 35/60/5 nylon 6/ABS/IA. The polyamide phase is stained dark by phosphotungstic acid (PTA).

5. Conclusions

The fracture toughness of nylon 6/ABS blends compatibilized with an IA polymer was examined by Izod and SEN3PB type tests. The SEN3PB specimens were tested as a function of the ligament length to determine the limiting specific fracture energy, u_o, and the dissipative energy density, u_d, which potentially are equivalent to the parameters w_e and βw_p in the essential work of fracture, EWF, methodology developed by Mai et al. Compatibilized SEN3PB specimens containing 5 wt.% IA were found to be tougher than nylon 6 or ABS over a broad range of ABS contents, with a maximum toughness observed at about 47.5 wt.% ABS. A dual mode of fracture was observed in SEN3PB specimens whose corresponding Izod specimens had ductile–brittle transition temperatures near room temperature (20 wt.% ABS). Ductile failure occurred in specimens with short ligament lengths, whereas specimens with longer ligaments deformed in a brittle manner. The critical ligament length at which the ductile-to-brittle transition occurred was found to be dependent on specimen thickness. A broader range of ligaments were ductile in thinner specimens, which can be rationalized in terms of a plane–strain to plane–stress transition in these materials. The fracture behavior of blends that were super tough as judged by Izod impact testing and had low ductile–brittle transition temperatures were found to be relatively insensitive to specimen thickness and were ductile over the entire range of ligament lengths.

The fracture properties of these blends were also affected by the compatibilizer content. Blends containing less than 2 wt.% IA exhibited dual modes of fracture, whereas blends containing 2 wt.% IA or higher of IA were fully ductile. Increasing the compatibilizer content did not cause large changes in the specific fracture energy for a given ligament length; however, a statistical analysis suggests that these small differences are statistically significant.

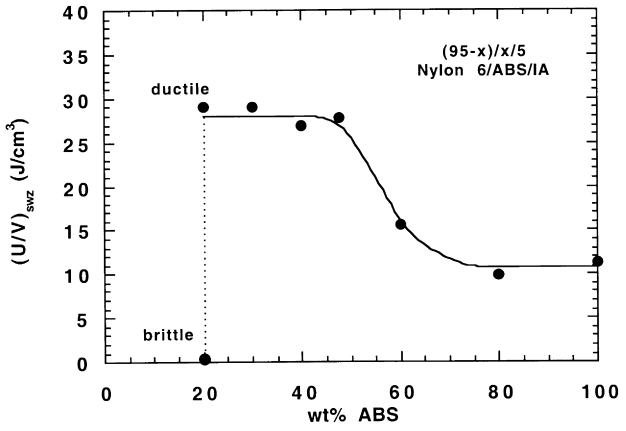

Fig. 17. Effect of ABS content on energy absorbed per unit volume in the stress-whitened zone, $(U/V)_{swz}$, for (95-x)/x/5 nylon 6/ABS/IA blends and pure ABS. Values of $(U/V)_{swz}$ were calculated using Eq. (11) and data from Fig. 15.

The stress-whitened zones of ductile SEN3PB specimens were found to be geometrically similar and independent of the original ligament length of the specimen. However, when comparing different ductile specimens, the amount of energy absorbed during plastic deformation (as judged by the value of u_d) was not always simply proportional to the size of the stress-whitened zone. In general, compatibilized blends containing higher amounts of nylon 6 were found to absorb more energy per unit of stress whitened material than ABS-rich compositions. This behavior appears to be related to differences in the primary deformation mechanisms that can occur in these blends.

Acknowledgements

This research was supported by the Army Research Office. The authors are indebted to AlliedSignal, Rohm and Haas and Cheil Industries for providing materials. Special thanks are due to Dr. C.B. Bucknall, Dr. K.M. Liechti and Dr. D.M. Himmelblau for their many helpful discussions.

References

[1] Aoki Y, Watanabe M. Polym Engng Sci 1992;32:878.
[2] Baer M. US Patent No. 4584344, 1986 (assigned to Monsanto).
[3] Lavengood RE, Silver FM. Soc Plast Engng ANTEC 1987;45:1369.
[4] Lavengood RE, Padwa AR, Harris AF. US Patent No. 4713415, 1987 (assigned to Monsanto).
[5] Misra A, Sawhney G, Kumar RA. J Appl Polym Sci 1993;50:1179.
[6] Triacca V, Keskkula H, Paul DR. Polymer 1991;32:1401.
[7] Majumdar B, Keskkula H, Paul DR. Polymer 1994;35:3164.
[8] Majumdar B, Keskkula H, Paul DR. Polymer 1994;35:5453.
[9] Majumdar B, Keskkula H, Paul DR. Polymer 1994;35:5468.
[10] Kudva RA, Keskkula H, Paul DR. Submitted for publication.
[11] Kudva RA, Keskkula H, Paul DR. Submitted for publication.
[12] Padwa AR, Lavengood RE. Polym Prepr Am Chem Soc, Div Polym Chem 1992;33:600.
[13] Carrot C, Guillet J, May JF. Plast Rubb Comp Proc Appl 1991;16:61.
[14] Kim BK, Lee YM, Jeong HM. Polymer 1993;34:2075.
[15] Howe DV, Wolkowicz MD. Polym Engng Sci 1987;27:1582.
[16] Crouch BA, Huang DD. J Mater Sci 1994;29:861.
[17] Duffy J, Shih CF. Proceedings of the Seventh International Conference on Fracture (ICF7). Oxford: Permagon, 1989. p. 633.
[18] Hashemi S, Williams JG. J Mater Sci 1991;26:621.
[19] Huang DD, Williams JG. J Mater Sci 1987;22:2503.
[20] Huang DD. Proceedings of the Seventh International Conference on Fracture (ICF7). Oxford: Permagon, 1989. p. 2725.
[21] Huang DD. The application of the multispecimen *J*-integral technique to toughened polymers. In: Joyce JA, editor. Elastic-plastic test methods: the user's experience, 2. Philadelphia, PA: ASTM, 1991.
[22] Seidler S, Grellmann W. J Mater Sci 1993;28:4078.
[23] Zhou Z, Landes JD, Huang DD. Polym Engng Sci 1994;34:128.
[24] E-813 Standard test method for J_{1c}, a measure of fracture toughness. Annual book of ASTM standards. Philadelphia, PA: ASTM.
[25] Williams JG. Fracture mechanics of polymers. New York: Ellis Horwood, 1984.
[26] Vu-Khanh T. Polymer 1988;29:1979.
[27] Mai Y-W, Powell P. J Polym Sci: Polym Phy 1991;29:785.
[28] Broberg KB. J Mech Phys Solids 1971;19:407.
[29] Broberg KB. J Mech Phys Solids 1975;23:215.
[30] Vu-Khanh T, de Charentenay FX. Polym Engng Sci 1985;25:841.
[31] Vu-Khanh T. Theor Appl Fracture Mech 1994;21:83.
[32] Hourston DJ, Lane S, Zhang HX. Polymer 1995;36:3051.
[33] Kayano Y, Keskkula H, Paul DR. Polymer 1997;38:1885.
[34] Kayano Y, Keskkula H, Paul DR. Polymer 1998;39:821.
[35] Kayano Y, Keskkula H, Paul DR. Polymer 1998;39:2385.
[36] Wu J, Mai YW. Polym Engng Sci 1996;36:2275.
[37] Wu J, Mai YW, Cotterell B. J Mater Sci 1993;28:3373.
[38] Mai YW, Cotterell B. Engng Fracture Mech 1985;21:123.
[39] Mai YW, Cotterell B. Int J Fracture 1986;32:105.
[40] Mai YW, Cotterell B, Horlyck R, Vigna G. Polym Engng Sci 1987;27:804.
[41] Hashemi S. J Mater Sci 1993;28:6178.
[42] Hashemi S. J Mater Sci 1997;32:1563.
[43] Hashemi S. Polym Engng Sci 1997;37:912.
[44] Levita G, Parisi L, Marchetti A. J Mater Sci 1994;29:4545.
[45] Levita G, Parisi L, Marchetti A. J Mater Sci 1996;31:1996.
[46] Karger-Kocsis J, Czigany T. Polymer 1996;37:2433.
[47] Karger-Kocsis J, Czigany T, Moskala E. Polymer 1997;38:4587.
[48] Karger-Kocsis J, Czigany T, Moskala E. Polymer 1998;39:3939.
[49] Paris PC, Tada H, Zahoor A, Ernst H. An initial experimental investigation of the tearing instability theory. In: Landes JD, Begley JA, Clarke GA, editors. Elastic–plastic fracture, ASTM STP 668, Philadelphia: ASTM, 1979.
[50] Paris PC, Tada H, Zahoor A, Ernst H. Instability of the tearing mode of elastic–plastic crack growth. In: Landes JD, Begley JA, Clarke GA, editors. Elastic–plastic fracture, ASTM STP 668, Philadelphia, PA: ASTM, 1979.
[51] Test Protocol for Essential Work of Fracture (Version 5). European Structural Integrity Society, 1997.
[52] Mai Y-W. In: Paul DR, Bucknall CB, editors. Polymer blends: formulation and performance. New York: Wiley, 1999 in press.
[53] Wildes G, Keskkula H, Paul DR. Submitted for publication.
[54] Hale W, Keskkula H, Paul DR. Polymer 1999;40:3353.
[55] Majumdar B, Keskkula H, Paul DR, Harvey NG. Polymer 1994;35:4263.
[56] Haldden-Abberton M. Polym Mater Sci Engng 1991;65:361.
[57] Kudva RA. Ph D Dissertation, University of Texas at Austin, 1999.
[58] Okada O, Keskkula H, Paul DR. Submitted for publication.
[59] Srawley JE, Gross B. Stress-intensity factors for single edge-notch specimens in bending or combined bending and tension by boundary collocation of a stress function. Technical note D-2603, NASA.
[60] Broek D. Elementary engineering fracture mechanics. Leiden: Noordoff, 1974.

[61] Hertzberg RW. Deformation and fracture mechanics of engineering materials, 4. New York: Wiley, 1996.
[62] Draper NR, Smith H. Applied regression analysis. New York: Wiley, 1998.
[63] Montgomery DC, Peck EA. Introduction to linear regression analysis. New York: Wiley, 1982.
[64] Borggreve RJM, Gaymans RJ, Eichenwald HM. Polymer 1989;30:78.
[65] Bucknall CB. Makromol Chem, Macromol Symp 1988;20/21:425.
[66] Fukui T, Kikuchi Y, Inoue T. Polymer 1991;32:2367.
[67] Majumdar B, Keskkula H, Paul DR. J Polym Sci: Polym Phys 1994;32:2127.
[68] Ramsteiner F, Heckmann W. Polym Commun 1985;26:199.
[69] Speroni F, Castoldi E, Fabbri P, Casiraghi T. J Mater Sci 1989;24:2165.
[70] Ben Jar P-Y, Wu RY, Kuboki T, Takahashi K, Shinmura T. J Mater Sci 1997;18:1489.
[71] Castellani L, Frassine R, Pavan A, Rink M. Polymer 1996;37:1329.
[72] Donald AM, Kramer EJ. J Mater Sci 1982;17:1765.
[73] Hagerman E. J Appl Polym Sci 1973;17:2203.
[74] Ni BY, Li JCM, Berry VK. Polymer 1991;32:2766.
[75] Bernal CR, Frontini PF, Sforza M, Bibbo MA. J Appl Polym Sci 1995;58:1.